Buried Optical Waveguide in Photo-Thermo-Refractive Glass by Ion Exchange Technology

Yinlei Hao, Jinwei Liu, Lufeng Che, Shiyong Wang, Haoran Meng, and Xinyue Liu

***Abstract*— To realize application of functional material Photo-Thermo-Refractive (PTR) glass for integrated photonic device production, PTR glass material is fabricated and employed as matrix material for planar optical waveguide manufacturing. Buried optical waveguide, with a core dimension of 8.7 μm × 9.0 μm (width by height), and its front edge located at approximately 12.5 μm underneath the glass substrate surface, is obtained by using thermal ion exchange (TIE) and subsequent field-assisted ion migration (FAIM). Transmission loss of these waveguides can be reduced to a value as low as 0.08 dB/cm at the operating wavelength of 1550 nm, and the coupling loss to standard single-mode-fiber is measured to be 0.47 dB/facet, demonstrating the feasibility of low-loss integrated photonic devices fabrication on PTR glass materials by ion exchange technology.**

***Index Terms*— Glass, integrated optics, optical waveguide.**

I. Introduction

PHOTO-THERMO-REFRACTIVE (PTR) glasses is a novel category of functional material that possess a specific refractive index modulation of amplitude as high as 10^{-3} upon UV exposure and subsequent thermal development, due primarily to precipitated NaF nanocrystals dispersed in the glass matrix [1], [2], [3]. Owing to their unique characteristics of high amplitude of refractive index modulation, excellent thermal stability, and high transparency in the visible and infrared range, PTR glasses have found extensive applications as matrix materials for the fabrication of various volume Bragg grating that serve as wavelength selective elements in the construction of high-performance lasers [4], spectroscopies, 3-D display instruments and augmented reality (AR) display devices [5] as well. Moreover, PTR glasses are expected to play an important role in the fabrication of strong Bragg grating devices in fiber [6] and integrated photonic devices [7], [8], [9], [10], [11], [12], among which planar Bragg grating in integrated photonic chip is the most anticipated.

Planar optical waveguides are the building block of integrated optical circuits, and thus the fabrication of high-performance optical waveguides on PTR glass substrates is one of key issues that need to be addressed. In the last decade, at least four approaches have been attempted by different researchers to optical waveguide fabrication on PTR glass substrate. Firstly, ion implantation technique, with doping ions of proton [7], helium [8] or carbon [9], among other species, has been employed by the Chun-Xiao Liu group. However, ion implantation techniques usually produce optical waveguides of high transmission loss, typically 4.28 dB/cm at the operating wavelength of 632.8 nm [9], due mainly to scattering at surface defects generated in the ion implantation process. Secondly, femtosecond laser irradiation has been tried for the fabrication of optical waveguide in PTR glass substrate, and waveguide with transmission loss of 0.6 dB/cm at the operating wavelength of 632.8 nm has been reported [10], [11], but the efficiency of this method is limited to some extent, due to the serial nature of the production process. The third approach is electron beam irradiation, while no information on waveguide propagation loss is reported [12]. Last but not least, ion exchange, a proven approach for planar optical waveguide fabrication in glass substrate for devices utilized for both optical communication [13] and optical interconnects [14], [15], has also been applied on PTR glass substrate, and surface optical waveguides have been achieved, with transmission loss on the order of 0.5 dB/cm in the visible range [16]. However, to the best of our knowledge, buried optical waveguide, which is highly expected in integrated photonic devices for its low loss characteristics, has not been produced in PTR glass substrate by ion exchange.

In the letter, aiming at further reduction of optical waveguide transmission loss in PTR glass substrate and thus pave the way for the application of this new category of functional material in integrated photonic device fabrication, a study on buried optical waveguide fabrication by ion exchange technology is conducted. Results exhibit that buried optical

Manuscript received 23 January 2023; revised 29 March 2023; accepted 10 May 2023. Date of publication 16 May 2023; date of current version 6 June 2023. This work was supported in part by the Basic Research Projects of Shenzhen Virtual University Park (Free Exploration Type) under Grant 2021Szvup155; in part by the National Natural Science Foundation of China under Grant 12173073; in part by the National Key Research and Development Program of China under Grant 2021YFB3202603; in part by the Key Research and Development Program of Jilin Province under Grant 20180201050SF; and in part by the Open Project Program of the Key Laboratory of Infrared System Detection and Imaging Technology, Chinese Academy of Sciences. *(Corresponding author: Yinlei Hao.)*

Yinlei Hao is with the College of Information Science and Electronic Engineering, Zhejiang University, Hangzhou 310027, China, and also with the Shenzhen Institute, Zhejiang University, Shenzhen 518057, China (e-mail: haoyinlei@zju.edu.cn).

Jinwei Liu and Lufeng Che are with the College of Information Science and Electronic Engineering, Zhejiang University, Hangzhou 310027, China (e-mail: 22231039@zju.edu.cn; lfche@zju.edu.cn).

Shiyong Wang is with the Key Laboratory of Infrared System Detection and Imaging Technology, Chinese Academy of Sciences, Shanghai 200083, China (e-mail: s_y_w@sina.com).

Haoran Meng and Xinyue Liu are with the Changchun Institute of Optics, Fine Mechanics and Physics, Chinese Academy of Sciences, Changchun 130033, China (e-mail: menghaoran@ciomp.ac.cn; liuxinyue@ciomp.ac.cn).

Color versions of one or more figures in this letter are available at https://doi.org/10.1109/LPT.2023.3276758.

Digital Object Identifier 10.1109/LPT.2023.3276758

waveguides, with transmission loss as low as 0.08 dB/cm, and coupling loss of 0.47 dB/facet can be obtained in the PTR glass substrate.

II. Experiments

PTR glass material of SiO_2-Al_2O_3-ZnO-Na_2O-NaF system, doped with Ag_2O, $CeO_2$and Sb_2O_3, is employed for optical waveguide fabrication. The glass batch is melted at 1500 °C in the air atmosphere in a platinum crucible settled in an electric furnace, and a platinum mechanical stirrer is applied to mechanically minimize striae content. The glass transition temperature Tg of the glass is measured to be 470 °C with a differential scanning calorimeter. The refractive index of the glass material at 1550 nm is measured to be 1.4833. The PTR glass batch is cut into disc-shaped wafers of 76.2 mm in diameter and 1.0 mm in thickness, and these wafers are polished to optical grade on both sides.

The precipitation behavior of NaF nanocrystals in the PTR material upon UV irradiation and subsequent thermal treatment was characterized by means of X-ray diffraction (XRD). A UV LED with wavelength of 305 nm and power of 30 mW is utilized as the irradiation source, and the irradiation dose on PTR glass is regulated to 1.0 W/cm^2.

Silver ion doping by Ag^+/Na^+ ion exchange is selected for optical waveguide forming, due primarily to the high mobility of Ag^+ in glass material at elevated temperatures, and the convenience of waveguide refractive index contrast regulation as well.

The manufacturing of optical waveguides is completed by two stages, thermal ion exchange (TIE), and subsequent field-assisted ion migration (FAIM). Channel waveguide layout in the glass wafer is defined by ion exchange windows lithographically formed in the aluminum mask film, which is physically deposited on the glass wafer surface. In the current experiments, ion exchange windows are 3.0 μm in width. The TIE is conducted at 280 °C in a muffle furnace, the glass wafer being immersed in a molten salts mixture of $AgNO_3$, $NaNO_3$ and $Ca(NO_3)_2$ in a silica container, $Ca(NO_3)_2$ being induced to lower the melting temperature of the salts mixture. In this process, silver ions from the molten salt mixture enter the glass substrate and form a diffusion zone adjacent to the glass wafer surface, and simultaneously, a part of sodium ions in the glass substrate adjacent to the ion exchange windows enter the molten salts mixture. After the completion of the TIE, the aluminum mask film on the glass wafer surface is removed by wet etching, and silver ion doped zones are formed in the surface layer of the glass wafer.

In the process of FAIM, the second stage of waveguide fabrication, a DC voltage is applied across the glass wafer at 260 °C to form a DC electric field in its thickness direction, and doping silver ions in the glass wafer migrate into the inner part of the glass wafer from its surface layer, driven by this DC electric field. In order to establish a stable and uniform electric field in the glass wafer, two separated parts of molten salt mixtures, which can form good electrical contact with the glass wafer, were used respectively as conducting medium on the two sides of the glass wafer. Two platinum wires immersed in the two parts of salt mixtures are connected

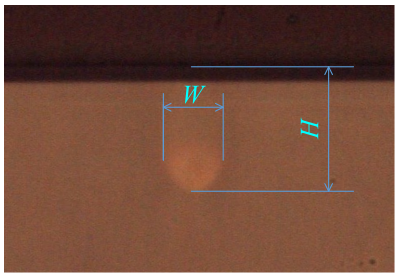

Fig. 1. Optical micrograph of the waveguide cross-section.

respectively to the positive and negative electrodes of the DC power supply. At the beginning of FAIM process, the DC power supply operates in the constant-voltage mode, and after the current flowing through the wafer reaches 60 mA, the DC power supply is converted to the constant-current mode, to prevent the glass wafer from being broken by Joule heat temperature rise effect generated by the electric current flowing through [17], [18].

The silver ion doped region in the glass substrate has a higher refractive index, forming the core of the channel waveguide, and the refractive index contrast is proportional to the concentration of silver ions that replaced the indigenous sodium ions in the glass matrix. In the current fabrication process, the waveguide refractive index contrast and geometric parameters, waveguide width and depth, as defined in Fig. 1, can be engineered by regulating the fabrication parameters. The waveguide refractive index contrast is principally governed by silver ion concentration in the molten salts mixture, TIE duration, and TIE temperature as well. The optical waveguide width W depends mainly on the width of the ion exchange window, as well as the TIE duration and temperature. It is worthy mentioning that W continues to increase during the FAIM process due to the diffusion of silver ions. FAIM is therefore conducted at a temperature lower than the TIE temperature, to slow down the waveguide widening rate and highlight the silver ions drifting motion deep into the glass substrate. The optical waveguide front edge depth H depends on many experimental parameters, including temperature and duration of TIE and FAIM, as well as the voltage across the glass wafer. Fortunately, it is found that the depth of the optical waveguide front is linearly related to the charge flux per unit area on the glass substrate during FAIM by

$$H = H_0 + M \int_0^T i_d\,(t)\,dt,$$

where H_0 is 3.1μm, and M is 0.56 C·cm^2·μm, for the conditions aforementioned; $i_d(t)$ is the current density that flowing through the glass wafer in the FAIM process, given as current per square centimeter as a function of time variable t; and T is the FAIM duration. Therefore, control of H can be achieved by monitoring the charge flux through the glass wafer.

III. Results and Discussions

The X-ray diffraction patterns of PTR glass after UV irradiation and heat treatment at 490 °C for 1 hour and 520 °C for 2 hours, respectively, are given in Fig. 2. The

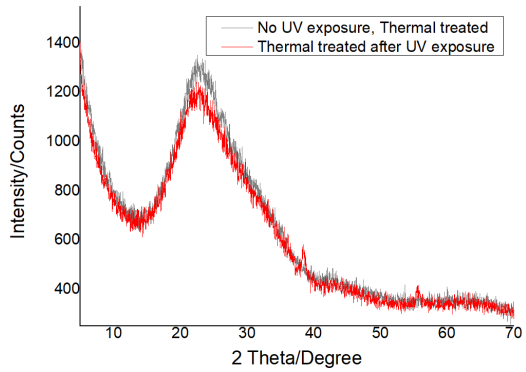

Fig. 2. XRD patterns of PTR glass with different treatment.

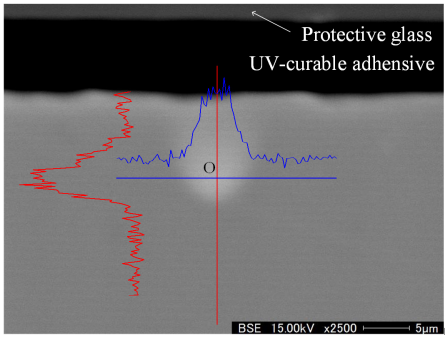

Fig. 3. BSE image of waveguide cross-section. The red curve in the graph gives the silver element content along the red vertical line, and the blue curve gives silver content along the blue horizontal line.

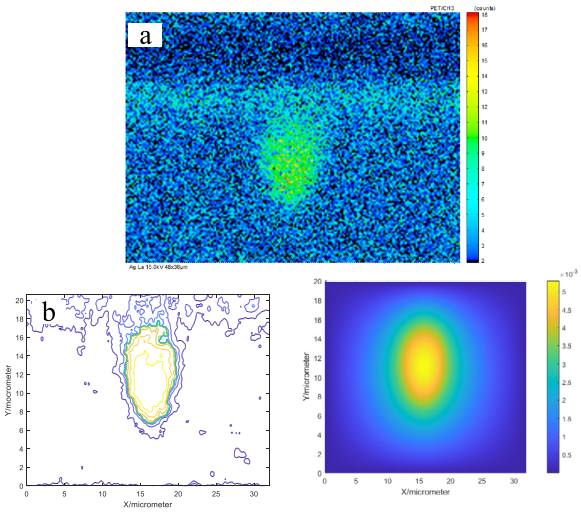

Fig. 4. Silver ion concentration profile (a), refractive index profile (b) and mode field profile (c) on the cross-section of the optical waveguide.

diffraction peaks located at 38.5 and 55.65 degrees correspond respectively to the (200) and (220) crystal plane diffraction of NaF crystals. The size of the NaF crystal can be estimated to be around 19.0 nm according to the Scherrer formula. From the diffraction pattern, it can be seen that NaF nanocrystals are precipitated in the glass matrix after UV exposure and subsequent heat treatment. As a contrast, the diffraction pattern of the glass undergoing the same heat treatment but with the absence of UV exposure is also given in the same figure. It can be seen that no distinguishable diffraction peak is found, suggesting no NaF crystal precipitation in the glass matrix with the absence of UV exposure, a typical property of PTR glass materials.

After the waveguide fabrication process is completed, a protective glass with the same radius as the wafer is glued to the glass wafer on its waveguide side with UV-curable adhesive. Then the wafer is cut into optical waveguide chips. After both end surfaces of the optical waveguide chips are ground and polished to optical grade for electron probe micro-analyzer (EPMA) and insertion loss test.

Cross-section of the channel optical waveguide is observed and characterized under an EPMA. Fig. 3 gives the backscattering electron (BSE) image of the optical waveguide cross-section under the EPMA. The comet-shaped region with greater brightness inside the glass matrix is the silver ion doped region formed after the TIE and FAIM process. It can be seen clearly that the silver ion doped region has been driven into the interior of the glass matrix. The dimension of silver doped zone is approximately 8.7 μm $\times$ 9.0 μm (width by height), with its front edge located at 12.5 μm underneath the glass surface. In the optical waveguide cross-section, silver element concentration along the vertical (red) and horizontal (blue) straight lines in the figure was respectively scanned by a wavelength dispersion spectrometer (WDS), with silver element concentration profiles being shown by the red and blue curves respectively. Moreover, silver content at point O, the intersection of the red line and the blue line in Fig. 3, is quantitatively estimated to be 0.4 at% by energy dispersive x-ray (EDX) analysis. Based on the semi-empirical formula of the refractive index and composition of the glass material [19], the refractive index increment at point O is approximately 0.0051.

The WDS is further utilized to obtain the silver ion concentration map over the optical waveguide cross-section, the result being shown in Fig. 4(a). According to the Ag concentration map and the linear relationship between glass refractive index and the extent of ion exchange, the waveguide refractive index profile is estimated, with result shown in Fig. 4(b). On this basis, the mode field of the waveguide fundamental mode, as that shown in Fig. 4(c) is calculated by numerically solving the corresponding scalar Helmholtz equation. Based on these measurements and calculations, the mode-field mismatch loss between the optical waveguide and the single-mode fiber SMF28 is estimated to be 0.43 dB/facet.

Insertion loss of the fabricated channel waveguides is measured by butt-coupling two single-mode fibers respectively to the two ends of the optical waveguide chip under test, and optical waveguide transmission loss and coupling loss between the waveguide and single-mode optical fiber is determined by the cut-back method. It is worth noting that the chip end face is reground and polished to optical grade after each cut of the chip. The dependence of optical waveguides insertion loss at wavelength 1550 nm on its length is given in Fig. 5. A linear fit to these data yields a waveguide transmission loss of 0.08 dB/cm, and a coupling loss of 0.47 dB/facet between the optical waveguide and the fiber. It is worth mentioning that the experimentally obtained glass optical waveguide transmission loss is significantly lower than the transmission loss of the channel optical waveguide on the PTR glass substrate reported in the existing literature. In fact, this value of transmission

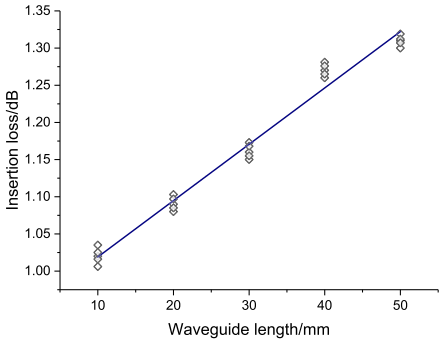

Fig. 5. Dependence of insertion loss on waveguide length.

loss corresponds to an internal transmittance of 98.2% per cm, which is close to the internal transmittance of optical glass materials. This is attributed to the fact that the silver ion doped zone in the fabricated optical waveguide is located below the surface of the glass substrate, and therefore the scattering loss at defects such as microcracks on the glass substrate surface can be completely eliminated. At the same time, the optical field profile of the buried waveguide is better matched to the optical field of the optical fiber than that of the surface waveguide, therefore coupling loss between the optical waveguide and the optical fiber can be effectively reduced.

IV. Conclusion

In conclusion, PTR glass material of SiO_2-Al_2O_3-ZnO-Na_2O-NaF system is fabricated, and buried optical waveguide is fabricated by TIE and FAIM techniques on the PTR glass substrate. Due primarily to elimination of scattering loss at glass substrate surface defects, transmission loss of these optical waveguides is reduced to 0.08 dB/cm at the operating wavelength of 1550 nm, a value close to the internal transmittance of the glass material itself; the coupling loss between this optical waveguide and single-mode fiber is about 0.47 dB/facet due to the high degree of mode-field matching between the waveguide and the single-mode fiber. It is demonstrated that buried optical waveguides with low transmission loss and coupling loss can be fabricated on PTR glass material, and therefore demonstrating the possibility of functional integrated photonic devices fabrication in PTR glass material substrate.

Acknowledgment

The authors would like to express their sincere thanks to Prof. Can Rao and Prof. Suwen Qiu, at the School of Earth Sciences, Zhejiang University, for their generous help in the EPMA characterization of the optical waveguide cross-section.

References

[1] J. Lumeau and E. D. Zanotto, "A review of the photo-thermal mechanism and crystallization of photo-thermo-refractive (PTR) glass," *Int. Mater. Rev.*, vol. 62, no. 6, pp. 348–366, Aug. 2017.

[2] S. Ivanov, V. Dubrovin, N. Nikonorov, M. Stolyarchuk, and A. Ignatiev, "Origin of refractive index change in photo-thermo-refractive glass," *J. Non-Crystalline Solids*, vol. 521, Oct. 2019, Art. no. 119496.

[3] E. Rotari, L. Glebova, and L. Glebov, "Refractive index modulation in photo-thermo-refractive fibers," *Proc. SPIE*, vol. 5709, pp. 379–384, 2005, doi: 10.1117/12.591217.

[4] V. Smirnov et al., "Ultranarrow bandwidth moiré reflecting Bragg gratings recorded in photo-thermo-refractive glass," *Opt. Lett.*, vol. 35, no. 4, pp. 592–594, 2010.

[5] S. B. Odinokov et al., "Augmented reality display based on photo-thermo-refractive glass planar waveguide," *Opt. Exp.*, vol. 28, no. 12, pp. 17581–17594, 2020.

[6] P. Hofmann et al., "Strong Bragg gratings in highly photosensitive photo-thermo-refractive-glass optical fiber," *IEEE Photon. Technol. Lett.*, vol. 25, no. 1, pp. 25–28, Jan. 1, 2013.

[7] J.-Y. Chen, Z.-H. Xie, W.-N. Li, S.-B. Lin, L.-L. Zhang, and C.-X. Liu, "Construction and investigation of a planar waveguide in photo-thermal-refractive glass by proton implantation," *Optik*, vol. 207, Apr. 2020, Art. no. 164461.

[8] S.-Q. Lin, L.-J. Shen, M. Tang, R.-L. Zheng, Q.-Y. Yue, and C.-X. Liu, "Characterization of optical planar waveguide formed by helium ion implantation in PTR glass," *Indian J. Phys.*, vol. 96, no. 13, pp. 3961–3965, Nov. 2022.

[9] Y. Wang et al., "Optical planar waveguides in photo-thermal-refractive glasses fabricated by single- or double-energy carbon ion implantation," *Opt. Eng.*, vol. 57, Jan. 2018, Art. no. 017103.

[10] Z. Zhang et al., "Nd^{3+}: Photo-thermo-refractive glass waveguides written by femtosecond laser," *Acta Photon. Sin.*, vol. 48, no. 3, p. 15, 2019.

[11] Y. J. Zhang et al., "Double line and tubular depressed cladding waveguides written by femtosecond laser irradiation in PTR glass," *Opt. Mater. Exp.*, vol. 7, no. 7, pp. 2626–2635, 2017.

[12] A. A. Zhiganov et al., "Forming optical waveguides in silicate glasses under electron irradiation," *J. Opt. Technol.*, vol. 78, no. 10, pp. 684–686, 2011.

[13] Y. Hao et al., "Single-mode-fiber-matched waveguide by silver/sodium ion-exchange and field-assisted ion-diffusion," *Optoelectron. Adv. Mater. Rapid Commun.*, vol. 3, no. 9, pp. 865–868, 2009.

[14] L. Brusberg et al., "Glass substrate with integrated waveguides for surface mount photonic packaging," *J. Lightw. Technol.*, vol. 39, no. 4, pp. 912–919, Feb. 15, 2021.

[15] J. Schwietering et al., "Integrated optical single-mode waveguide structures in thin glass for flip-chip PIC assembly and fiber coupling," in *Proc. IEEE 70th Electron. Compon. Technol. Conf. (ECTC)*, Jun. 2020, pp. 148–155.

[16] Y. M. Sgibnev, N. V. Nikonorov, V. N. Vasilev, and A. I. Ignatiev, "Optical gradient waveguides in photo-thermo-refractive glass formed by ion exchange method," *J. Lightw. Technol.*, vol. 33, no. 17, pp. 3730–3735, Sep. 1, 2015.

[17] Y. Hao et al., "Experiments and analysis on Joule heating effect in field-assisted ion diffusion," *Opt. Eng.*, vol. 51, no. 1, 2012, Art. no. 014601.

[18] Y. Hao et al., "Simulation of field-assisted ion-migration process for glass-based PLC fabrication: Influence of Joule heat effect," *J. Optoelectron. Adv. Mater.*, vol. 19, nos. 3–4, pp. 197–203, 2017.

[19] S. D. Fantone, "Refractive index and spectral models for gradient-index materials," *Appl. Opt.*, vol. 22, no. 3, pp. 432–440, 1983.